Research Article

Crystal Growth and Characterization of p-Arsanilic Acid for Pharmaceutical Application with Theoretical Conformational Study

M. Sangeetha, R. Mathammal*, R. Mekala
Department of Physics, Sri Sarada College for Women(Autonomous), Salem, Tamilnadu, India.
***Corresponding author's E-mail:** mathammals_shanmugam@yahoo.com

Accepted on: 02-07-2015; **Finalized on:** 31-08-2015.

ABSTRACT

p-Arsanilic acid, which is otherwise known as 4-amino phenyl arsonic acid, is a bioactive compound. Single crystals of p-Arsanilic acid (pAsA) are grown successfully under slow evaporation technique. The crystallinity and parameters of the grown crystal are determined with the powder x-ray diffraction result. The functional groups are characterized by FTIR and FT-RAMAN spectra. The UV spectrum reveals its application in the optoelectronic field. The molecular structure of the title compound is studied using density functional theory (DFT). The vibrational frequencies and the potential energy distribution (PED) are calculated using DFT/B3LYP 6-31+G** basis set. The stability of the molecule is determined by various conformers in the computational method. The HOMO-LUMO (Highest Occupied Molecular Orbital – Lowest Unoccupied Molecular Orbital) charge transfer and Non-Linear Optical (NLO) property determination were carried out. The electrophilic and nucleophilic attack of the molecule is studied using the MEP (Molecular Electrostatic Potential).

Keywords: Characterization; Single crystal growth; Computer simulation; Arsanilic acid.

INTRODUCTION

The physical properties of the solid state seen in crystals and powders of both drugs and pharmaceutical excipients are of interest because they can affect both the production of dosage forms and the performance of the finished product. The nature of the crystalline form of a drug may affect its stability in the solid state, its solution properties and its absorption. In order to study the stability and bioactivity of the title pharmaceutical compound, it is chosen for crystal growth and its properties are studied theoretically in detail.

The use of arsenic and its compounds are very popular in the production of pesticides, herbicides and insecticides. They are used as food additives in the poultry and swine industries in developing countries.[1-3]

As a food additive; they control disease, simulate growth and improve both feed efficiency and conversion in animals. Majority of the organoarsenic compounds are not metabolized in the poultry and are excreted chemically unchanged and the manure is turned into fertilizer pellets for commercial use.

After the application of the fertilizer to soil, microbial activity and the presence of ultraviolet light lead to the formation of other organic arsenic species.[4-6] This in turn poses a number of health and environmental concerns. Since arsenic, in its various forms, is a known Carcinogen[7-11] it has been correlated with hypertension as well as other cardio metabolic diseases.[12]

Arsanilic acid is used in the laboratory, for instance in recent modification of nanoparticles. It is also launched in chemotherapeutic approach for treating infectious diseases of human beings.

Density Functional Theory (DFT) is an effective cum economical tool for studying the structural properties of the molecule. Spectroscopic techniques eminently help in determining the dynamic behaviour of the electronic and molecular structures of natural products at microscopic level.[13,14] In this work, DFT technique is employed to study the complete vibrational spectra of p-Arsanilic acid.

Crystal growth and Characterization techniques

The pure sample of p-Arsanilic acid is purchased from Spectro. Chem Ltd, Mumbai, India and used as such for crystal growth. From the solubility test, sodium carbonate solution is found to be the good solvent. To the 50ml of sodium carbonate solution, the titled substance is dissolved up to the supersaturated state. Then the solution was filtered and kept undisturbed for slow evaporation. The nucleation began after 30 days. A single crystal of 20 x 10 x 5 mm^3 size was harvested at the seventh week. The transparency of the crystal is shown in Figure 1.

Figure 1: Grown crystal of p-Arsanilic acid

The grown crystal is subjected to powder x-ray diffraction studies to reveal the crystallinity of the substance. The powdered sample is scanned in the range 10–90°C at a scan rate of 2°/min using the JEOL JDX services instrument with CuKα (λ = 1.5406A˚) radiation. The room temperature FTIR spectrum of the title compound is measured in the region 4000-400 cm^{-1} with the scanning speed of 10 cm^{-1} min^{-1} and the spectral resolution of 4.0 cm^{-1} by employing Perking-Elmer spectrometer. The FT-Raman spectrum of the compound is recorded using Bruker FRA 106/S instrument equipped with Nd: YAG laser source operating at 1064 nm line widths with 100mW power. The spectrum is recorded in the range of 4000–10 cm^{-1}. ^{1}H and ^{13}C NMR (400 MHz; DMSO) spectra are recorded using BRUKER TPX-400 FT-NMR spectrometer. The optical absorption spectrum is recorded using Perkin-Elmer Lamda 935 UV-VIS-NIR spectrometer. The non-linear optical activity of the compound is determined using Kurtz powder technique.

Computational Details

Density functional theory (DFT) is extensively used due to their accuracy and low computational cost to calculate a wide variety of molecular properties and provided reliable results which were in accordance with experimental data. The molecular structure of pAsA and corresponding vibrational harmonic frequencies are calculated using Becke3-Lee-Yang-Parr (B3LYP) with 6-31+G** basis set using GAUSSIAN 09W[15] program package.

Electronic properties: HOMO-LUMO energies, absorption wavelengths and oscillator strengths are calculated using B3LYP method, based on the optimized structure in gas phase. Moreover, the dipole moment, linear polarizabilities, and hyper polarizabilities are also studied. 1H and 13C chemical shifts were calculated with GIAO approach[16] by applying B3LYP/6-31+G** method.

RESULTS AND DISCUSSION

Powder X-Ray Diffraction studies

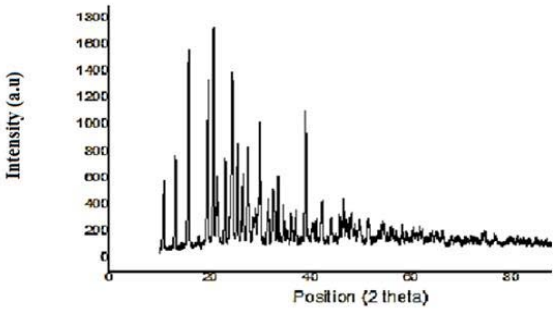

Figure 2: Powder X-ray diffraction pattern of pAsA crystals

The powder x-ray diffraction analysis helps in determining the crystalline nature of the grown crystal. Using the JEOL JDX services instrument with CuKα (λ = 1.5406A˚) radiation the sample is scanned with the range 10–90°C at a scan rate of 2°/min. The crystal belongs to monoclinic type and the lattice parameters obtained from the Powder XRD data are given below.

a = 7.241 (2), b = 6.214(1), c = 8.643(1), β = 101.19(1)°, V= 381.5 (1) A^{o3}

The crystallinity of pAsA is well defined by the prominent peaks at specific 2θ values which can be seen in Figure 2.

Conformational Stability and Molecular geometry

In order to determine the most stable structure of p-AsA, the energies of various conformers were calculated. The optimization was performed for the most stable conformer with global minimum energy. The molecular geometry of the title compound is described on the basis of bond lengths, bond angles and dihedral angles. The compound under investigation belong to C_1 point group symmetry with the global minimum energy E=-2747.732 Hartree. The optimized structure reveals that pAsA to be zwitter ionic form and it is shown in Figure 3. The C-C bond length for pAsA calculated at B3LYP/6-31+G** level lies in the range 1.3883 to 1.4106 A^0. This coincides with the analogous molecule whose C-C bond length varies from 1.358 to 1.491 A^0.[17] The presence of electronegative arsenic atom has reduced the calculated C-N bond length and it slightly varies from the experimental value (1.47 A^0).[18] The substitution of arsenic in the ring exerts a valence electron cloud of nitrogen atom resulting in an increase force constant and decrease in bond length. The bond length between carbon and arsenic is probably large due to the electronegative nature of the arsenic. The As14-O15 and As14-O17 bond lengths, have the values 1.7702 and 1.7825 A^0, which coincides with the analogous molecule respectively.[19] The As14-O19 bond distance is reduced to 1.63 A^0 because of the inductive effect of the amino group. The O15-H16 bond and O17-H18 bond takes the value 0.9699 and 0.9705 A^0 respectively, which coincide with the analogous molecule.[20]

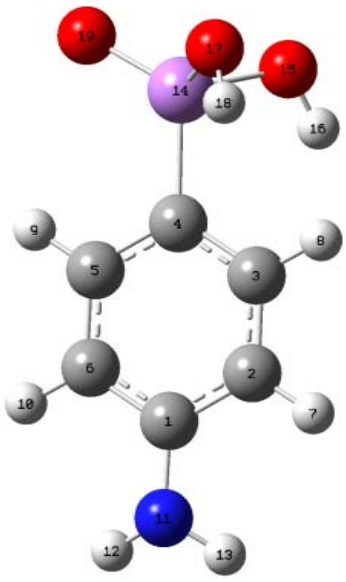

Figure 3: Optimized structure of p-AsA with atom numbering

The distortion in the ring is mainly due to the substituents and its consideration is very important. Among the six angles of ring, the angle C6-C1-C2 and C5-C4-C3 have a slight variation because of the presence of amine and arsenic group. The geometry optimization performed on the title compound indicates that it exhibits intramolecular hydrogen bond interaction. The magnitude of the bond angles O15-As14-O17 and O19-As14-O17 are 98.72^{o} and 111.24^{o} respectively, which indicates that As14-O17 is not symmetrically disposed on As14 and tilted towards O19 atom to form H-bonding between O19 and H18 atoms. The magnitude of the bond angles C1-N11-H12 and C1-N11-H13 is 117.6 and 117.70^{o} respectively, which indicates that C1-N11 bond, is symmetrically disposed on C1.

Vibrational Analysis

A complete vibrational assignment for the title compound is obtained using Gauss view program. The potential energy distribution (PED) illustrates the frequency distribution for the molecule under study. Most of the calculated frequencies are in coincidence with the available data. The optimized structure of pAsA comes under C_1 symmetry and has 51 normal modes of vibrations. The observed and calculated frequencies are summarised in the Table 1. The experimental and calculated FTIR spectra and FT-RAMAN spectra are shown in Figure 4 and 5.

C-C vibrations

Generally, the C-C stretching vibration occurs in the region 1625-1430cm^{-1}. The actual position of these modes is determined not so much by the form of substituents but by the form of substitution around the ring.[21] The bands at 1571 cm^{-1}, 1414 cm^{-1}, 1289 cm^{-1}, 1096 cm^{-1} in the IR and 1289cm^{-1}, 1094cm^{-1} in Raman are assigned for CC stretching. The corresponding calculated frequencies take the values 1575, 1542, 1400, 1282, 1066cm^{-1}. The in-plane vibration is at higher frequency than the out-of-plane vibration, which is due to the substituent group. The ring vibrations are observed at 516, 610, 616 cm^{-1} in IR, 614cm^{-1} in Raman and their corresponding calculated frequencies are 514, 592 and 620cm^{-1}. The ring torsional deformation vibrations are predicted at 726, 415 and 72cm^{-1}, which are active in Raman.

C-H vibrations

The aromatic C-H stretching vibrations are normally found between 3100 and 3000 cm^{-1}. In this region, the bands are not affected appreciably by the nature of the substituents. The CH stretching mode is assigned to the peak at 2802, 2905 and 3033cm^{-1} in the IR and the Raman active modes are at 2993, 3061 and 3150cm^{-1}. The calculated frequencies at 3069, 3065 and 3042 cm^{-1} also depict the CH stretching vibrations.

The region 1300-1000cm^{-1} is expected for CH in-plane bending vibrations. Similarly for the title molecule the bands at 1326 and 1140 cm^{-1} are allotted for in-plane bending in IR spectrum. The CH out - of - plane vibrations is expected in the range 1000-700 cm^{-1}. For this molecule, the peak at 976 cm^{-1} is assigned for out –of –plane bending vibration and the calculated frequencies are 970 and 990cm^{-1}.

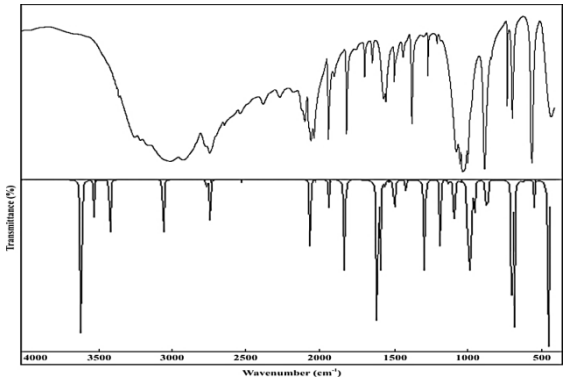

Figure 4: Comparison of observed and B3LYP/6-31+G** calculated FTIR spectra of p-Arsanilic acid

As-O vibrations

The As-O stretching and bending vibrations are expected to appear in the region 1000-300 cm^{-1}.[22] However, the calculated band located at 928 cm^{-1} is assigned to the stretching mode of As-O band. The bond distance of As-OH types are 1.78 and 1.77A^{o}. The greatest distance corresponds to the lowest wavenumbers at 670 and 651 cm^{-1}. The bands due to symmetric and asymmetric bending vibrations are identified in the 550-400 cm^{-1} frequency region in IR spectra. Two bands located at 319 and 282 cm^{-1} are assigned to asymmetric bending mode, whereas the symmetric mode appears at 136 cm^{-1}.

O-H and N-H vibrations

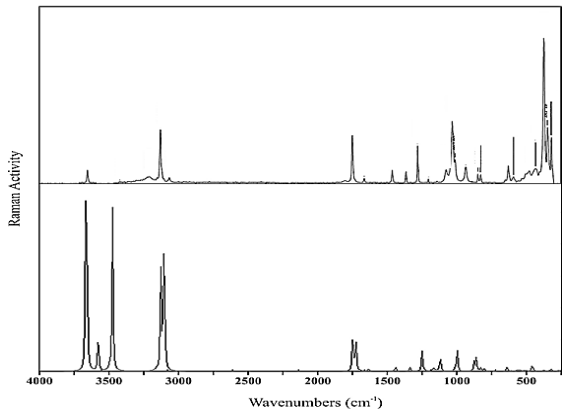

Figure 5: Comparison of Observed and B3LYP/6 - 31+G**Calculated FT-RAMAN

In dilute solutions, O-H stretching appears as a sharp band at higher frequency around 3600 cm^{-1} due to free O-H group. In spectra of undiluted liquids or solids, intermolecular hydrogen bonding broadens the band and shifts its position to lower frequency (3200–3500 cm^{-1}).[23] The peak at 3603cm^{-1} in Raman is assigned to O-H stretching and the calculated frequency also falls at 3633cm^{-1} with 100% PED contribution. The OH bending

vibrations are observed in the region 965 and 948 cm^{-1} which coincides with the experimental data.

It is stated that in amines, the N-H stretching vibrations occur in the range 3400-3300 cm^{-1}.[24] With reference to this, the vibrational frequencies observed at 3482 in Raman and 3405 in IR are assigned to NH stretching modes. The peak observed at 1234 cm^{-1} is allotted for C-NH_2 stretching mode.

The in-plane –NH_2 bending vibration falls from 1650-1580 cm^{-1}. The IR peak at 1602 cm^{-1} and Raman peak at 1594cm^{-1} is allotted for NH_2 bending vibration. Likewise, the out- of- plane bending -NH_2 band at 826 cm^{-1} in the IR 830 cm^{-1} in Raman is assigned to the amino group deformation mode.

Table 1: Observed and B3LYP/6-31+G** level calculated vibrational frequencies (in cm^{-1}) of p-Arsanilic acid

Observed frequencies (in cm^{-1})		Calculated frequencies (in cm^{-1})		IR intensity	Raman intensity	PED(%)
		Unscaled frequencies	Scaled frequencies			
-	-	21	20	0.3095	3.3950	τHOAsC(92)
-	72	83	80	1.3174	3.2423	τring(44),δAsCCC(35), δOCOAs(15)
-	101	102	97	3.0357	0.9722	δAsCC(43),δOCOAs(20), βOAsO(11)
-	130	142	136	44.0230	1.9336	δOAsO(39),τHOAsC(36), βAsCC(11)
-	-	177	169	4.0025	0.2230	δOCOAs(26), τring(22)
-	192	228	218	21.8340	1.5824	τHOAsC(39), δOAsO(27)
-	241	233	223	23.5420	9.8303	νAsC(35),βOAsO(29)
-	-	282	269	25.0923	1.2246	δOCOAs(44),βOAsO(13),τHOAsC(11)
-	-	295	282	31.7708	1.5450	βOAsO(43), τHOAsC(24)
-	-	334	319	117.3647	2.8311	βOAsO(54), νAsC(13)
-	-	349	334	104.0826	1.3573	τHOAsC(28), δAsCCC(14)
-	-	352	337	54.6721	0.9138	δOCOAs(28) δAsCCC(14)
-	-	354	339	7.7920	0.1847	τHNCC(83)
-	362	406	388	0.2051	1.0149	βNCC(64), βAsCC(10)
-	401	435	416	330.4568	8.7377	βHNCC(83)
-	415	436	417	1.4405	0.0717	τring(79),τNCCC(10)
516	-	537	514	16.2490	0.5584	βring(54), τHOAsC(17)
610	-	619	592	2.7211	4.5056	βring(54), νAsC(23)
616	613	649	620	1.6575	5.4753	βring(79)
636	634	681	651	130.2023	24.6207	νAsO(93)
-	-	701	670	130.6002	15.7532	νAsO(94)
744	726	773	739	0.2750	0.1604	τring(48), τNCCC(22)
-	-	835	799	14.0495	25.8755	νCC(28), τHCCN(22), νCN(13)
-	808	838	801	2.1537	8.1850	τHCCN(63), τHCCC(11)
826	830	848	810	47.5682	3.2203	τHCCN(57), τHCCC(14)
-	-	971	928	41.1559	18.3490	νAsO(74) ,βHOAs(18)
		992	948	111.4965	1.9601	βHOAs(95)
975	-	1009	965	138.4029	1.9005	βHOAs(57), νAsO(19)
976	-	1014	970	7.0007	0.0720	τHCCC(51), τHCCN(20), τring(12)
-	-	1025	980	18.6809	7.2956	βHCC(40), νCC(22)
-	-	1037	992	0.5479	0.1766	τHCCC(56), τHCCN(20), τring(18)
1019	1012	1071	1024	0.4095	0.4537	βHNC(62), νCC(22)
1096	1094	1115	1066	75.6260	33.3023	νCC(49), νCAs(16)
-	-	1156	1105	3.5097	0.5701	βHCC(47), νCC(27)
1140	-	1215	1162	39.2371	5.9179	βHCC(72)
1234	-	1328	1269	101.4780	7.8833	νCN(51)
-	1289	1341	1282	10.4023	1.1439	νCC(39), βHCC(33)
1326	-	1372	1312	1.1265	0.3068	βHCC(24)νCC(23), βHCN(14)
1414	-	1465	1400	6.2808	0.2752	νCC(40), βHCC(31)

1474	-	1545	1477	58.6103	3.1089	βHCC(53)
-	-	1613	1542	9.2024	1.2640	νCC(71)
1571	-	1647	1575	72.1447	49.1366	νCC(37), βHNH(20)
1602	1594	1670	1596	265.0262	48.4841	βHNH(68)
2820	-	3182	3042	11.7466	100.3993	νCH(91)
2905	2993	3183	3043	11.7947	91.5474	νCH(98)
3033	3061	3206	3065	4.7684	86.0142	νCH(99)
-	3150	3210	3069	3.5663	102.8208	νCH(92)
3405	-	3595	3437	52.4562	263.5943	νNH(100)
-	3482	3709	3506	26.5557	64.5784	νNH(100)
-	3603	3799	3633	101.1245	89.7011	νOH(99)
-	-	3805	3638	99.7559	227.7897	νOH(99)

ν – Stretching, β – bending, δ –out of plane, τ – torsion, PED- Potential Energy Distribution.

NMR Analysis

NMR serves as a great resource in determining the structure of an organic compound by revealing the hydrogen and carbon skeleton. Chemical shifts of pAsA are determined experimentally and the theoretical chemical shifts are predicted using Gauge – Invariant Atomic Orbitals (GIAO). The ^{1}H atom is mostly localized on periphery of the molecules and their chemical shifts would be more susceptible to inter molecular interactions in the aqueous solutions as compared to that of other heavier atoms. The chemical shift (δ) value provides information on the magnetic/chemical environment of the protons. Protons next to electron withdrawing groups are deshielded, whereas protons next to electron-donating groups are shielded.[25] The hydrogen atoms attached to the electron withdrawing oxygen atom in the hydroxyl group decrease the shielding. This results in the low chemical shift for the hydroxyl protons. Whereas, the protons attached to the ring are in the range 6.87-8.04 ppm and the experimental values also fall in the same range coinciding with the theoretical data. Usually aromatic carbons possess the chemical shift values from 100-150 ppm. Due to the influence of electronegative nitrogen atom, the chemical shift value of C1 of pAsA is significantly differing in the shift position and the corresponding value is 151.08 ppm.

Frontier Molecular Orbitals

The analysis of the wave function indicates that the electron absorption corresponds to a transition from the ground state to the excited state and is mainly described by one electron excitation from the HOMO to LUMO. Both HOMO and LUMO are the main orbital taking part in chemical reaction. HOMO energy characterizes the capability of electron giving; LUMO characterizes the capability of electron accepting.[26] The frontier orbital gap helps to characterize the chemical reactivity, optical polarizability, chemical hardness and softness of a molecule.[27] The surfaces for the frontier orbital are drawn to understand the bonding scheme of the title compound. Two important molecular orbital (MO) were examined for the title compound, the highest occupied molecular orbital (HOMO) and the lowest unoccupied molecular orbital (LUMO) are given in Figure 6. The calculated HOMO and LUMO energies are -0.23498eV and -0.03750eV and the resulting band gap energy is 0.19748eV. The chemical stability of a molecule is determined by the hard and soft nature of it. HOMO-LUMO energy gap helps to find whether the molecule is hard or soft. Hard molecules have large energy gap and soft molecules have small energy gap. The soft molecules are more polarizable than the hard ones because they need small energy for excitation. The hardness value of a molecule can be determined as η = (-HOMO+LUMO)/2. The value of η of the title molecule is 0.13624eV. Hence, it shows that the title compound belongs to soft material.

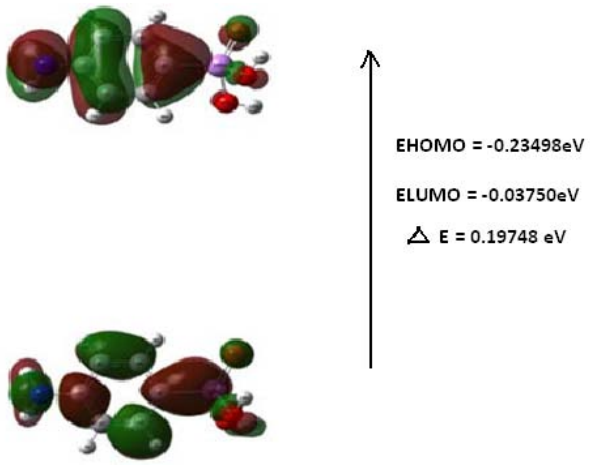

Figure 6: The atomic orbital compositions of the frontier molecular orbital for p-Arsanilic acid

UV-Vis Spectra Analysis

The grown crystal is subjected to UV-Vis-NIR spectral analysis and the lower cut-off wavelength is found to be 240nm. The wide transparency region in the visible and NIR region proves the molecule to be a good one for optical applications. Energy gap of pAsA is calculated by using the formula given below.

$$E = \frac{1.243 \times 10^3}{\lambda_{max}}$$

Where, λ is the lower cutoff wavelength and the energy gap value is found as 5.1375 eV. Time-dependent density functional theory (TD-DFT) calculation is performed for pAsA on the basis of fully optimized ground state structure to investigate the electronic absorption properties. The λ_{max} values which are the function of electron availability, electronic excitation energies and oscillator strength are obtained from the UV-Visible spectra, simulated theoretically with B3LYP/6-31+G** basis set. The calculated absorption maxima values for pAsA have been found to be 267.96, 263.03 and 260.36nm. The oscillator strength for 260.36 nm is of higher in magnitude compared to other transitions. The absorption band of pAsA at the longer wave length region 267.96nm is caused by the n – π* transition.

Molecular Electrostatic Potential

The molecular electrostatic potential (MEP) is used primarily for predicting sites and relative reactivities towards electrophilic attack, in studies of biological recognition and hydrogen bonding interactions. To predict the reactive sites for electrophilic and nucleophilic attack for pAsA, the MEP at the B3LYP/6-31+G** method is calculated as shown in Figure7. Different colours on the MEP represent the different values of the electrostatic surface. The electrostatic potential increases in the order red<orange<yellow<green<blue. The colour code of the maps is in the range between -4.056eV (deepest red) and 4.506eV (deepest blue) in the title molecule, where blue colour indicates the strongest attractions and red indicates strongest repulsion. The region of negative V(r) is associated with the lone pair of electrons.

As seen from the Figure 7, in the pAsA the amine group region has negative potential and As-OH region has positive potential. The predominance of the light green region of MEPs surface corresponds to a potential halfway between the two extremes red and dark blue colour. The positive (blue) region of MEP is related to electrophilic reactivity and the negative (red) regions to nucleophilic reactivity.

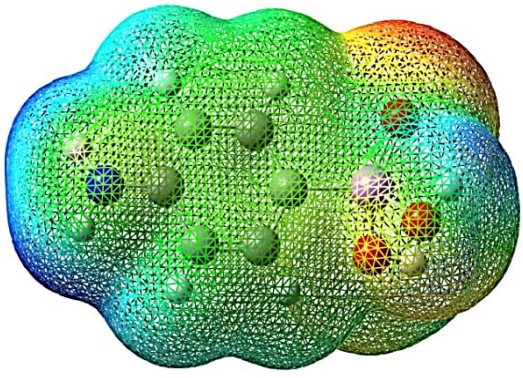

Figure 7: The total electron density isosurface mapped with molecular electrostatic potential of p-Arsanilic acid.

NLO studies

In order to confirm the enhancement of nonlinearity of pAsA, second harmonic efficiency test is performed by the modified version of powder technique developed by Kurtz and Perry.[28,29] The powdered sample of pAsA crystal is illuminated using the fundamental beam of 1064nm from Q-switched ND:YAG laser. The input pulse energy of 1.9 mJ/pulse and pulse width 8 ns and repetition rate of 10 Hz are used.

The second harmonic signal generated by the crystal was confirmed from the emission of green radiation of wavelength 532nm. The output voltage was 41mV and it was 0.5 times greater than the KDP value (76 mV).

In order to investigate the relationships between molecular structures and non-linear optical properties (NLO), the polarizibilities and first order hyperpolarizabilities of the pAsA compound are calculated using DFT/B3LYP method with 6-31+G** basis set, based on finite field approach.

The polarizability and hyperpolarizability tensors can be obtained by a frequency job output file of Gaussian. The mean polarizability(α_{tot}), anisotropy of polarizability($\Delta\alpha$) and the average value of the first order hyperpolarizability(β_{tot}) can be calculated using the equations:

$$\alpha_{tot} = \alpha_{xx} + \alpha_{yy} + \alpha_{zz} / 3$$

$$\Delta\alpha = 1/\sqrt{2}[(\alpha_{xx} - \alpha_{yy})^2 + (\alpha_{yy} - \alpha_{zz})^2 + (\alpha_{zz} - \alpha_{xx})^2 + 6\alpha^2_{xx}]^{1/2}$$

$$\beta = [(\beta_{xxx} + \beta_{xyy} + \beta_{xzz})^2 + (\beta_{yyy} + \beta_{yzz} + \beta_{yxx})^2 + (\beta_{zzz} + \beta_{zxx} + \beta_{zyy})^2]^{1/2}$$

The polarizability and hyperpolarizability are reported in atomic units(a.u), the calculated values have been converted into electrostatic units (esu) (for α : 1 a.u = 0.1482×10^{-24})esu, for β:1 a.u = 8.6393×10^{-33})esu.

The total dipole moment (μ) for the title compound can be calculated using the following equation.

$$\mu = (\mu_x^2 + \mu_y^2 + \mu_z^2)^{1/2}$$

It is well-known that the higher value of dipole moment, molecular polarizability and first order hyperpolarizability are important for more active NLO properties. The large value of hyperpolarizability, β which is a function of the non-linear optical activity of the molecular system is associated with the intra molecular charge transfer.

The physical properties of these conjugated molecules are governed by the high degree of electronic charge delocalization along with the charge transfer axis and by the low band gaps.

The calculated first order hyperpolarizability of the title compound is 6.258×10^{-30} esu, which is 48 times greater than that of urea (0.13×10^{-30}esu).[30]

So it is revealed that the title molecule is an attractive object for future studies of non-linear optical properties.

CONCLUSION

Single crystals of p-Arsanilic acid have been grown using the slow evaporation technique. The crystallinity and the cell parameters have been revealed by the powder XRD results. The detailed vibrational analysis has been studied using DFT/B3LYP method and most of the calculated frequencies coincide with the experimental FTIR and FT-RAMAN data. The UV studies show a wide transparency region above the lower cut-off region and large band gap energy. This proves the optical quality of the crystal. The emission of green radiation from the SHG studies is yet another proof for title compound to be a good NLO material. The stability, chemical reactivity, intramolecular interaction of the molecule are analysed with the help of theoretical calculations in detail. The molecular electrostatic potential surface (ESP) provides information regarding the size, shape, charge density distribution and sites of chemical reactivity of the title molecule. The intermolecular interactions in the compound is found out with the help of the reactive sites. A deep insight into the charge transfer is elucidated by NBO analysis. The correlations between the thermodynamics and temperature are also obtained.

Acknowledgement: The authors are sincerely thankful to the SHG measurement facility extended by Prof. P.K. Das, Department of Inorganic and physical chemistry, Indian Institute of Science, Bangalore. The authors are also thankful to Sophisticated Analytical Instrumentation Facility (SAIF), IIT, Chennai, and St. Joseph's College, Trichirappalli, India for providing spectral measurements.

REFERENCES

1. Jones F.T., A Broad View of Arsenic.oult, Sci, 86, 2007, 2-14 and references therein.
2. Cullen, W.R. Is Arsenic an Aphrodisiac? The sociochemistry of an Element, RSC Publishing, Cambridge, 2008.
3. Canadian Food Inspection Agency- Arsanilic acid (Date Revised 2006-09) http://WWW.inspection.gc.ca/animals/feeds/medicating-ingredients/mib/mib_4/eng/1330714521085/1330716893328.
4. Cortinas I.; Filed J.A.; Kopplin M., Garbarinco J.R.; Gandolfi A.J.; Sierra-Alvarez R., Anaerobic Biotransformation of Roxarsone and related N-Substituted Phenylarsonic acids. Environ. Sci.Technol, 40, 2006, 2951-2957.
5. Markris K.C.; Quazi M.; Pumamiya P.; Sarkar D.; Datta R, Fate of Arsenic in Swine Waste from concentrated Animal feeding Operations.J.Environ.Qual., 37, 2008, 1626-1633.
6. Jackson B.P.; Bertsch P.M., Determination of Arsenic speciation in Poultry wastes by IC-ICP-MS. Environ.Sci.Technol, 35, 2001, 4868-4873.
7. Bissena M.; Frimmel F.H, Arsenic-a Review Part I: Occurrence, Toxicity, Speciation, Mobility. ActaHydrochim, Hydrobiol, 31, 2003, 9-18.
8. Dopp. E; Hartmann L.M; Florea A.-M; Rettenmeier A.W.; Hirner A.V, Environmental Distribution, Analysis, and Toxicity of organometal (Loid) Compounds. Critical Rev. Toxic., 34, 2004, 301-333.
9. Kenyon E.M, A Concise Review of the Toxicity and Carcinogenicity of DimethylarsinicAcid.Toxicology, 160, 2001, 227-236.
10. Tchounwou P.B.; Centeno J.A.; Patlolla A.K. Arsenic Toxicity, Mutagenesis, and Carcinogenesis- a Health Risk Assessment and Management Approach. Mol.Cell.Biochem, 255, 2004, 47-55.
11. Hirano S.; Kobayashi Y.; Hayakawa T.; Cui X.; Yamamoto M.; Kanno S. Shraim, Accumalation and Toxicity of Monophenyl Arsenicals in Rat Endothelial Cells. Arch. Toxicol., 79, 2005, 54-61.
12. Abhyankar L.N.; Jones M.R.; Guallar E.; Navas-Acien, A. Arsenic Exposure and Hypertension: A Systematic Review. Environ. Health Perspect., 120, 2012, 494-500.
13. Srivastava A.; Tandon P.; Jain S.; AsthanaPoonamTandon B.P.; Sudha Jain B.P. Asthana, Antagonistic properties of a natural product – Bicuculline with the gamma-aminobutyric acid receptor: Studied through electrostatic potential mapping, electronic and vibrational spectra using ab initio and density functional theory, Spectrochim.Acta A, 84, 2011, 141-155.
14. Joshi B.D.; Srivastava A.; Tandon P.; Jain S.; Molecular structure, vibrational spectra and HOMO, LUMO analysis of yohimbine hydrochloride by density functional theory and ab initio Hartree–FockcalculationsSpectrochim.Acta A, 82, 2011, 270-278.
15. M.J.Frisch, 2009, Gaussian 09, Revision A.1, Gaussian, Inc., Wallingford CT.
16. Wolinski K.; Haacke R.; Hinton J.F; Pulay P.; Methods for parallel computation of SCF NMR chemical shifts by GIAO method: Efficient integral calculation, multi-Fock algorithm, and pseudodiagonalization, J.Comp.Chem. 18(6), 1997, 816-825.
17. Moreno-Fuquen R.,; Grajales-Tamayo M.; doP.Gambardella M.T.; The 1:1 Complex Formed by 2-Picoline N-Oxide and 3-Chlorobenzoic Acid, ActaCryst.C, 52, 1997, 1635.
18. Moreno-Fuquen R.; doP.Gambardella M.T.; deA.Santos R.H.; 1:1 Complex Formed by 2-Picoline N-Oxide and 4-Nitrophenol, ActaCryst. C, 52, 1996, 1745.
19. Adrian Adamescu, Ian Hamilton, Hind A. Al-badleh, Density functional theory calculations on the complexation of p-Arsanilic acid with hydrated iron oxide clusters: structures, reaction energies and transition states. J.Phys.Chem.A, 118(30), 2014, 5667-79.
20. L.J.Bellamy, The Infrared Spectra of Complex Molecules, (third ed.), Wiley, New York, 1975.
21. Gupta R.K.; Prasad R.; Bhatnagar H.L.; IR and laser Raman spectral studies on m-and p-(triufluoromethyl) benzoyl chloride and m-(chloromethyl) benzoyl chloride, Indian J.Pure Appl. Phys. 28 ,1990, 533-536.
22. Glenening E.D.; Reed A.E.; Carpenter J.E.; Weinhold F; NBO Version 3.1. TCI, University of Wisconsin, Madison, 1998.
23. P.S. Kalsi, Spectroscopy of Organic Compounds, sixth ed., New Age International (P) Limited Publishers, New Delhi, 2004.

24. Ben Ahmed A.; Feki H.; Abid Y.; Minot C.,; Molecular structure, vibrational spectra and nonlinear optical properties of orthoarsenic acid–tris-(hydroxymethyl)-aminomethane DFT study, SpectrochimicaActa Part A, 75, 2010, 1315-1320.

25. K. Fukui, Science 218, 1982, 747-754.

26. Kosar B.; Albayrak C.; Spectroscopic investigations and quantum chemical computational study of (E)-4-methoxy-2-[(p-tolylimino)methyl]phenolSpectrochim. Acta 78A, 2011, 160-167.

27. Luque F.J.; Lopez J.M.; Orozco M.; Perspective on "Electrostatic interactions of a solute with a continuum. A direct utilization of ab initio molecular potentials for the prevision of solvent effects" Theor.Chem.Acc. 103, 2000, 343.

28. Kurtz S.K.; Perry T.T.; A powder technique for the evaluation of nonlinear optical materials, J. Appl. Phys. 39, 1968, 3798–3813.

29. Franken P.A.; Hill A.E.; Peters C.W.; Weinreich G.; Generation of optical harmonics Phys. Rev. Lett. 7, 1961, 118–119.

30. Adant C.; Durpuis M.; Bredas J.L.; Ab initio study of the nonlinear optical properties of urea: Electron correlation and dispersion effects. Int.J.QuantumChem. 56, 1995, 497-507.

Source of Support: Nil, **Conflict of Interest:** None.